SCIENTIFIC REPORTS

OPEN

SUBJECT AREAS:
FLUORESCENCE IMAGING
LAB-ON-A-CHIP
CELL BIOLOGY
IMMUNOLOGY

Received
21 February 2014

Accepted
4 August 2014

Published
5 December 2014

Correspondence and requests for materials should be addressed to J.D. (jsdoh@postech.ac.kr) or K.-M.L. (kyunglee@korea.ac.kr)

* These authors contributed equally to this work.

Homotypic NK cell-to-cell communication controls cytokine responsiveness of innate immune NK cells

Tae-Jin Kim[1]*, Miju Kim[2,3]*, Hye Mi Kim[4], Seon Ah Lim[1], Eun-Ok Kim[1], Kwanghee Kim[1,6], Kwang Hoon Song[3], Jiyoung Kim[1], Vinay Kumar[5], Cassian Yee[6], Junsang Doh[2,3] & Kyung-Mi Lee[1,6]

[1]Global Research Lab, Department of Biochemistry and Molecular Biology, Korea University College of Medicine, Seoul 136-713, Korea, [2]School of Interdisciplinary Bioscience and Bioengineering (I-Bio), Pohang University of Science and Technology, Pohang, Gyeongbuk 790-784, Korea, [3]Department of Mechanical Engineering, Pohang University of Science and Technology, Pohang, Gyeongbuk 790-784, Korea, [4]Division of Integrative Biosciences and Biotechnology (IBB), Pohang University of Science and Technology, Pohang, Gyeongbuk 790-784, Korea, [5]Department of Pathology, University of Chicago, Chicago, IL 60637, USA, [6]Departments of Melanoma Medical Oncology and Immunology, MD Anderson Cancer Center Houston, TX 77054, USA.

While stationary organ cells are in continuous contact with neighboring cells, immune cells circulate throughout the body without an apparent requirement for cell-cell contact to persist in vivo. This study challenges current convention by demonstrating, both *in vitro* and *in vivo*, that innate immune NK cells can engage in homotypic NK-to-NK cell interactions for optimal survival, activation, and proliferation. Using a specialized cell-laden microwell approach, we discover that NK cells experiencing constant NK-to-NK contact exhibit a synergistic increase in activation status, cell proliferation, and anti-tumor function in response to IL-2 or IL-15. This effect is dependent on 2B4/CD48 ligation and an active cytoskeleton, resulting in amplification of IL-2 receptor signaling, enhanced CD122/CD132 colocalization, CD25 upregulation, and Stat3 activation. Conversely, 'orphan' NK cells demonstrate no such synergy and fail to persist. Therefore, our data uncover the existence of homotypic cell-to-cell communication among mobile innate lymphocytes, which promotes functional synergy within the cytokine-rich microenvironment.

As a first line of defense, natural killer (NK) cells play a critical role in eliminating acute infections and providing innate immune surveillance of tumor cells[1,2]. NK cells are activated upon recognition of down-regulated MHC class I and engagement of specific activating receptors including NKG2D, NK1.1, 2B4, DNAM-1, and natural cytotoxicity receptors (NCRs)[3]. Exposure to cytokines, such as IL-2, IL-12, IL-15, IL-18, and type I interferons promote NK cell priming and expansion[2,4]. While this model is generally accepted as the basis for NK cell activation and proliferation, it does not sufficiently explain the behavior of NK cells in culture, for example, the requirement for maintenance of a critical NK cell density during rapid *in vitro* expansion and the observation that highly purified NK cells grow faster and to larger numbers when cultured in round-bottom wells than in flat-bottom wells of similar dimensions. These observations would not be predicted by the general convention whereby NK cell activation and expansion are governed primarily by receptor pattern recognition and demonstrate that NK cells require homotypic cell-to-cell interaction.

To examine the contribution of NK cell-to-cell communication to the process of cell survival, activation, and proliferation, we adopted use of specialized cell-laden microwells under conditions where NK cells were grown in 'social microwells' (in which cells were allowed to contact each other freely), and 'lonesome microwells' (in which single-occupancy 'orphan' cells experience no cell-cell contact). By controlling the level of cellular proximity and their communication with neighboring cells, this system offers highly sensitive and quantifiable measurements of NK cell contact-mediated changes that cannot be obtained from a bulk population. Using this cell-laden approach, we now demonstrate that NK cells can utilize homotypic cell-to-cell contact for optimal activation, accelerated proliferation kinetics, and maximal effector functions via enhanced cytokine responsiveness that is dependent on 2B4/CD48 interaction.

Results

Highly purified NK cells proliferate to a significantly greater extent when cultured in round-bottom wells compared to flat-bottom wells in response to IL-2. Unlike T cells, NK cells can bypass antigen presenting cells

(APC)-mediated contacts and be fully activated in vitro using relatively high doses of IL-2[4]. Since IL-2/IL-2R signaling is not thought to be dependent on cell-cell contact, the initial seeding density of NK cells and surface area of wells in IL-2 would not be expected to affect the degree of activation. To test this, we purified NK cells from whole splenocytes, and cultured them in round or flat-bottom 96 well-plates with varying concentrations of IL-2 (Fig. 1a). To our surprise, NK cells in round-bottom wells demonstrated significantly higher levels of proliferation compared with those grown in flat-bottom wells at all doses of IL-2 tested, as measured by ^{3}H-thymidine incorporation and CFSE dilution assays (Fig. 1b–c). At the highest IL-2 dose, however, the growth difference between round- and flat-bottom wells became less apparent over time (day 6, Fig. 1c), indicating that high IL-2 concentrations can mitigate the enhancement seen in round-bottom wells. CD11b/CD27 staining[5] along with CFSE dilution assays revealed that peripheral NK cells at all stages of maturation ($CD11b^{low}CD27^{high} \rightarrow CD11b^{high}CD27^{high} \rightarrow CD11b^{high}CD27^{low}$) underwent higher levels of proliferation in round bottom wells than they did in flat-bottom wells (Fig. 1d), suggesting that cell to cell contact is important for the proliferation and survival of NK cells. Of note, NK cells with a more mature phenotype demonstrated a higher fold increase in proliferation in round-bottom wells than less mature NK cells.

The enhanced proliferation observed in round-bottom wells suggests that cell density, not the total number, of NK cells is important in controlling the rate of cell division. At a fixed IL-2 concentration of 500 U/mL (Fig. 2a), we found that NK cells in round-bottom wells achieved maximum proliferation after 5 days at the lowest cell concentration (0.1×10^5 cells, 82.6%, Fig. 2b), while cells cultured in flat-bottom wells yielded a proliferative fraction of only 50% at the lowest cell concentration, gradually increasing to a maximal level of proliferation only at the highest cell density (81.4% at 5×10^5 cells/well; Fig. 2b). When these events were assessed over time, NK cells in round-bottom wells consistently exhibited a higher percentage of CFSE-diluted cells from day 3 (Fig. 2c). Supporting the hypothesis that effective density is important, we observe, beginning at day 4, that an increase in the percentage of proliferating cells in flat-bottom wells correlates positively with cell number; in contrast, the increase in percentage of proliferating cells in round-bottom wells is cell number-independent. Therefore, NK cell-to-cell contacts may modulate proliferation kinetics by lowering the threshold of activation by IL-2.

NK cells in round-bottom wells demonstrate increased activation markers and responsiveness to IL-2 compared to flat-bottom wells. We next examined if increased NK cell proliferation by cell-cell contact correlated with the activation status of NK cells. Expression of the very early activation marker, CD69, and upregulation of IL-2Rα chain (CD25) were found to be significantly increased in NK cells cultured in round-bottom wells when compared to those in

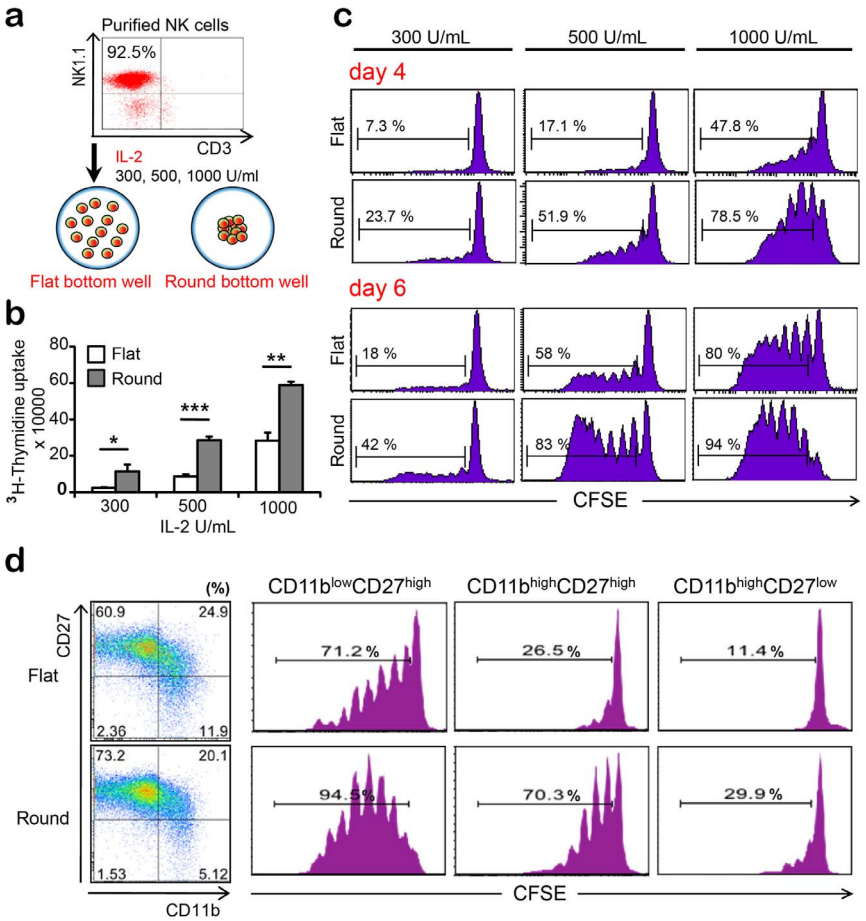

Figure 1 | NK cells in round-bottom wells exhibit higher proliferation than those in flat-bottom wells in response to IL-2. (a) Purified NK cells (0.5×10^5 cells/well) were cultured with IL-2 at 300, 500 or 1000 U/ml in flat-bottom or round-bottom wells in 96-well plates. (b) ^{3}H-thymidine incorporation assay to assess cellular proliferation was performed 4 days after the start of NK cell culture. Data are representative of five independent experiments. Error bars shown are SD from triplicates. (c) CFSE dilution assay was performed at 4 and 6 days after IL-2 stimulation of NK cells in flat or round-bottom wells. Fraction of NK cells undergoing cell division is shown for each histogram as percent of total NK cells in culture. Data are representative of three independent experiments. (d) CD11b/CD27 staining was performed along with CFSE dilution assay at 5 days after IL-2 stimulation (500 U/ml). One sample t-test was performed. * $p<0.05$, ** $p<0.01$, *** $p<0.001$.

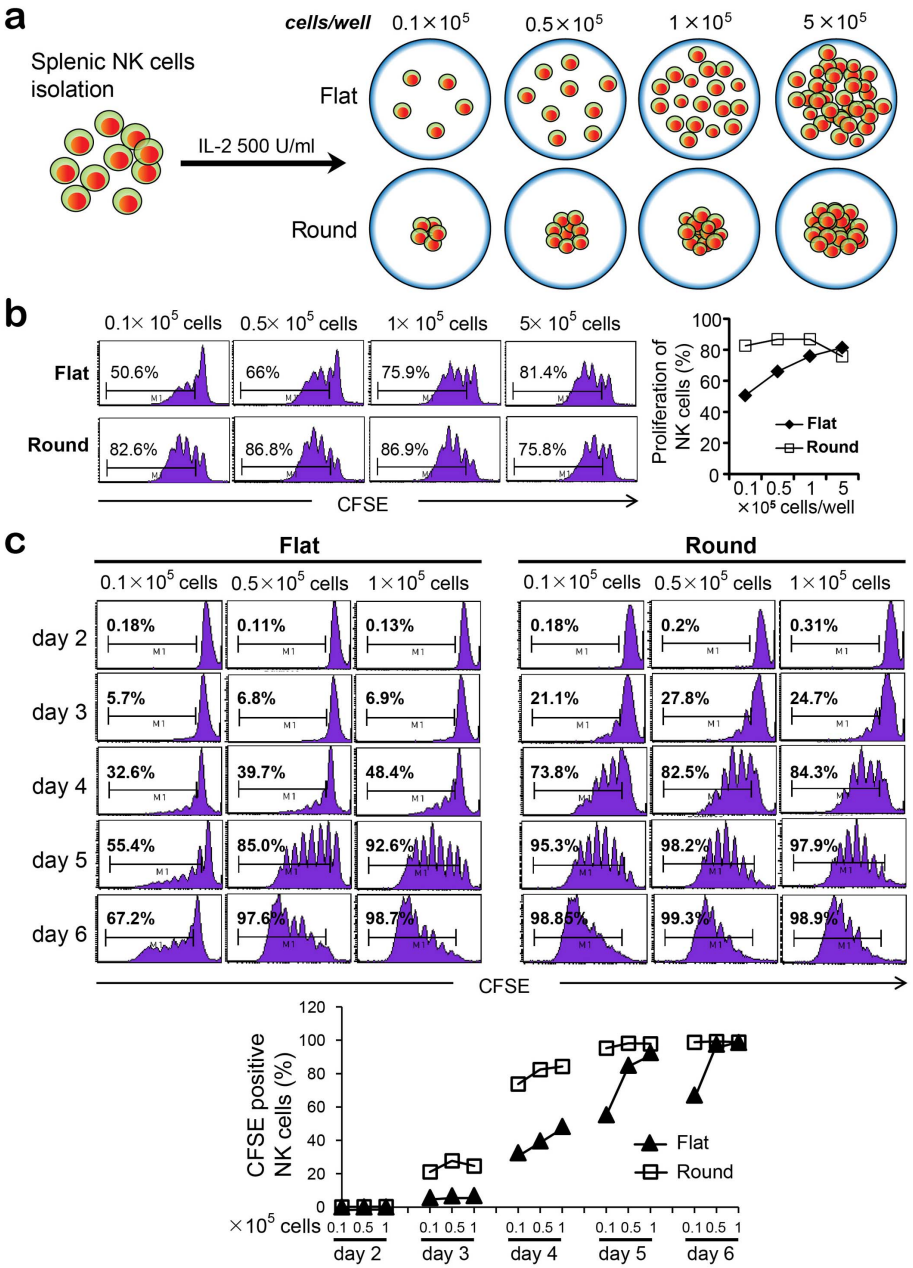

Figure 2 | Local density of NK cells is important for NK cell proliferation in response to IL-2. (a) Purified NK cells were plated onto flat- or round-bottom wells at 0.1×10^5, 0.5×10^5, 1×10^5, or 5×10^5 cells/well, and cultured with 500 U/ml IL-2. (b) NK cell proliferation as assessed by CFSE dilution assays was performed 5 days after 500 U/ml IL-2 treatment. (c) CFSE dilution assays were performed at the time indicated using various NK cell numbers. Fraction of NK cells undergoing proliferation is shown for each histogram as percent of total NK cells in culture. The data shown are representative of four independent experiments.

flat-bottom wells 3 days following exposure to a suboptimal dose of IL-2 (300 U/ml, Fig. 3a). The differences in CD25 and CD69 expression between NK cells cultured in round- vs. flat-bottom wells were apparent from day 2 and continued until day 4, after which it became indistinguishable. This may have been due to both cultures reaching a proliferative plateau by day 6, as seen in Fig. 2c, or to a difference in cell survival among NK cells between the two types of wells. To determine whether there was a difference in NK cell survival, we performed Annexin V and propidium iodide (PI) staining by flow cytometry as markers of apoptotic and necrotic cell death processes, respectively. While there was no significant difference in cell death between day 2 and day 4, significantly larger numbers of late-stage apoptotic cells (upper right quadrant, Annexin V^+PI^+) were found in the flat-bottom wells than in the round-bottom wells at day 6 (Fig. 3b). This result suggests that NK cells cultured in round-bottom wells, in which cells are in close proximity to each other and maintain cell-cell contact, exhibited enhanced survival by these measures when compared with cells cultured in flat-bottom wells.

We next asked whether this contact–mediated increase in activation and proliferation could lead to changes in NK cell effector functions. When NK cells cultured in round- or flat-bottom wells were admixed with NK-sensitive YAC-1 target cells, NK cells underwent degranulation and exposed CD107a (LAMP1) on the surface[6]. Among NK cells cultured in round-bottom wells, not only was there a higher percentage of $NK1.1^+$ cells expressing surface CD107a (6.3% vs. 11.9%), but these cells also expressed higher levels of surface CD107a (mean MFI: 17.5 vs. 26.41, upper panel; Fig. 3c). Similarly, both the percentage and level of intracellular IFN-γ expression was

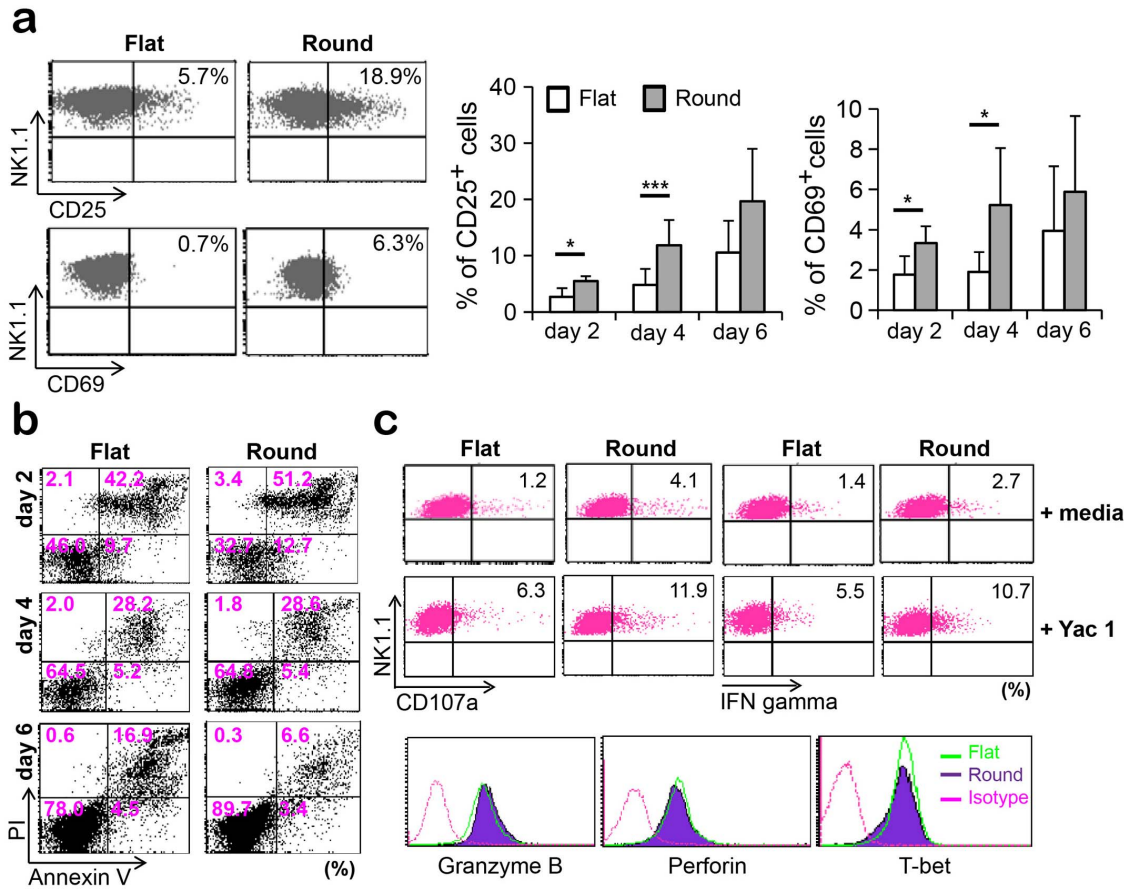

Figure 3 | NK cells in round-bottom wells exhibit higher activation status and greater cytotoxicity than those in flat-bottom wells. (a) Purified NK cells were plated onto flat- or round-bottom wells (0.5×10^5/well), treated with 300 U/ml of IL-2 for 36 h, and expression levels of activation markers (CD25 and CD69) analyzed by flow cytometry. (b) PI/Annexin V staining, assessed by flow cytometry, was performed at 2, 4, 6 days with NK cells plated as above. (c) NK cells upon stimulation by Yac-1 cells were analyzed for the expression of CD107a degranulation marker and IFN-gamma cytokine. Expression of granzyme B, perforin, and T-bet in NK cells cultured in round (solid curve) versus flat-bottom wells (open curve) were analyzed by flow cytometry prior to the stimulation with YAC-1 cells. The data shown are representative of 3 independent experiments. One sample t-test was performed. * $p<0.05$, *** $p<0.001$.

significantly elevated in NK cells cultured in round-bottom plates (5.5% vs 10.7%, mean MFI: 9.15 vs. 12.03; Fig. 3c). The differences in cytotoxicity and IFN-γ secretion observed between NK cells cultured in round vs. flat-bottom wells were not due to the differences in the intracellular levels of granzyme B or perforin (components of cytotoxic machinery), or T-bet, a transcriptional factor controlling IFN-γ production (bottom panels, Fig. 3c). Taken together, these data suggest that NK-NK cell contact can control not only the rate of proliferation, but also the activation status of NK cells resulting in elevated NK cell effector functions.

Homotypic cell-to-cell interaction results in increased CD122/CD132 cluster formation, as revealed by cell-laden 'social' and 'lonesome' microwells. The concept that cell-to-cell contact increases activation and proliferation in response to IL-2 prompted us to investigate the signaling pathways downstream of IL-2R. We adopted a recently developed "cell-laden microwell approach", where the effect of cell-cell contact can be precisely controlled and evaluated in a context-dependent fashion[7]. Cell-laden microwells containing three different sizes of microwells in a single surface were fabricated (Fig. 4a). In the 60 μm and 40 μm microwells, cells were allowed to contact each other; termed 'social' microwells. To prevent cell-cell contact, 4 by 4 arrays of 12 μm circular microwells, which correspond to the size of activated NK cells, termed 'lonesome' microwells were used. Importantly, a 40 μm social microwell contains ~16 cells on average, which approximates the number of cells contained in a 4 by 4 array of 'lonesome' microwells, while a 60 μm social microwell, holding ~ 33 total cells on average, occupies an area equivalent to that of a 4 by 4 array of lonesome microwells (Fig. 4a). When purified NK cells were cultured in IL-2 for 36 hours, cells in both 60 μm and 40 μm social microwells exhibited a higher proliferative index, as evidenced by elevated Ki-67 expression, than those in lonesome microwells (Fig. 4b). Similar upregulation of CD25 expression was observed on NK cells in social microwells after 36 h, confirming the activated status of NK cells compared with those in lonesome microwells (Fig. 4c). These data provide strong support for the hypothesis that contact-mediated NK-NK cell interactions control the degree of activation and proliferation of NK cells by IL-2.

Initial events upon IL-2 stimulation in naïve NK cells entail clustering of IL-2βR (CD122) and common γ (CD132) chains to drive low affinity IL-2R signaling. Therefore, we next examined if cell-to-cell contact modulated CD122/CD132 clustering in response to IL-2. As shown in Fig. 4d, NK cells cultured in both social and lonesome microwells demonstrated bright puncta of CD122 and CD132 that were more colocalized on the surfaces of cells, as a result of IL-2 stimulation. However, the number of colocalized CD122/CD132 puncta was significantly higher in cells cultured in social microwells than those in lonesome microwells, indicating that when NK cells are permitted to contact other NK cells, augmented clustering of

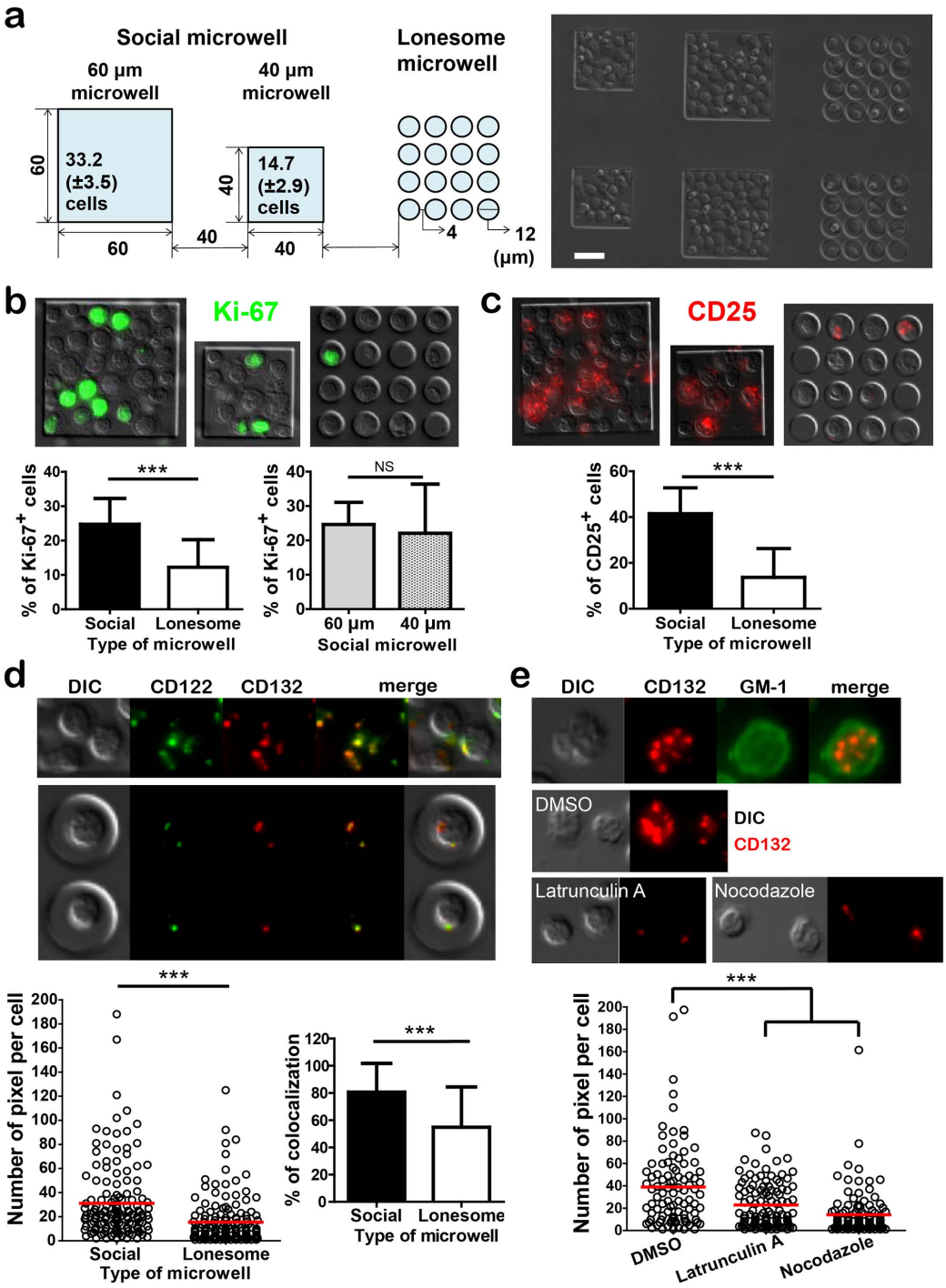

Figure 4 | Analysis of homotypic NK-NK interactions using cell-laden microwells. (a) Schematic illustration of microwells used (left) and a representative differential interference contrast (DIC) image of successfully fabricated NK cell-laden microwells. (right, scale bar: 20 µm). Various numbers of NK cells can be accommodated in 'social' microwells while only a single NK cell occupies a 'lonesome' microwell; therefore contact-mediated NK-NK interactions are permissible in social microwells, but restricted in lonesome microwells. NK cells were plated into microwells, treated with 500 U/ml of IL-2, and fixed at 18 h and 36 h prior to immunostaining. (b) NK cells were fixed at 36 h after IL-2 treatment and stained with FITC-Ki-67. Representative overlay images of DIC and fluorescence images (upper panels), and quantification of Ki-67$^+$ cells (lower panel) are shown. (c) NK cells were fixed at 36 h after IL-2 addition, and stained with PE-anti CD25 mAbs. Representative overlay images of DIC and fluorescence images (upper panels), and quantification of CD25$^+$ cells (lower panel). (d) NK cells were fixed at 18 h after IL-2 treatment, and stained with FITC-anti-CD122 and PE-anti-CD132 mAbs. Top, Representative fluorescence images for CD122 (green) and CD132 (red) Bottom, Quantification of CD122/CD132 cluster area/cell and colocalization of CD122/CD132 puncta. (e) Immunofluorescence microscopy of GM-1 was performed to assess the contribution of lipid rafts to CD122/CD132 clustering. Additionally, NK cells were treated with pharmacological inhibitors of actin and microtubule activity (Latrunculin A (10 µM) and Nocodazole (20 µM), respectively), stimulated in round-bottom wells with 500 U/ml of IL-2, and stained for CD132 to quantify CD132 clustering. Representative images of GM-1/CD132 co-staining (top), CD132 clustering of control (DMSO) and inhibitor-treated cells (middle), and quantification of CD132 clustering (bottom) are shown. Data are representative of 3 independent experiments. One sample t-test was performed. *** $p<0.001$.

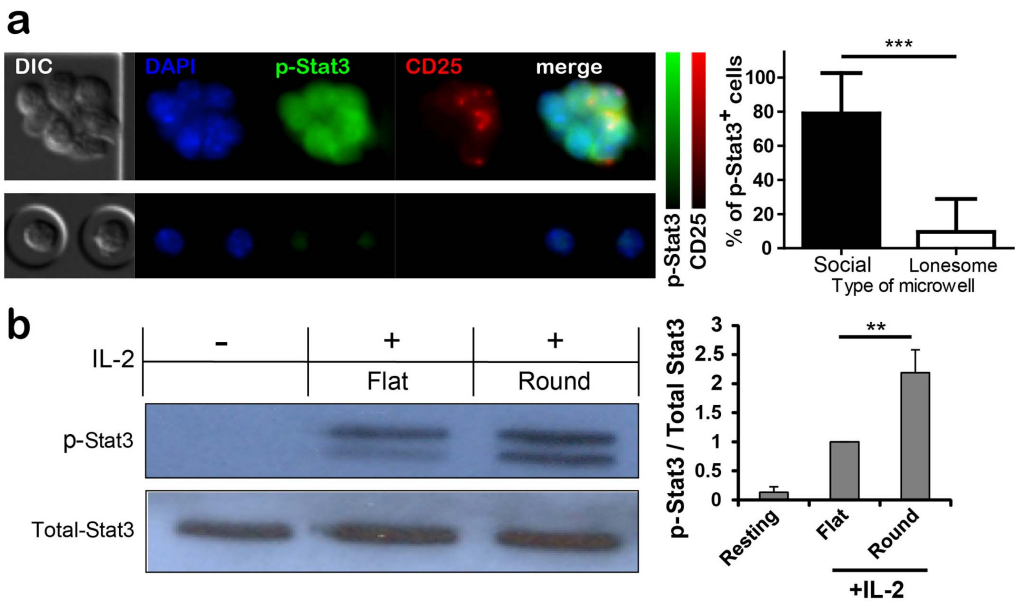

Figure 5 | NK cells in round-bottom wells or social microwells exhibit enhanced Stat3 phosphorylation than those in flat-bottom wells or lonesome microwells. (a) NK cells in social (top row) or lonesome (bottom row) microwells were treated with 500 U/ml of IL-2 for 18 h, fixed and stained with p-Stat3 and CD25. Representative fluorescence images for DAPI (blue), p-Stat3 (green) and CD25 (red) (left panel) and quantification of p-Stat3$^+$ NK cells (right panel). Data are representative of 3 independent experiments. (b) Western blot analysis of NK cells cultured in round- vs. flat-bottom wells using p-Stat3 and total-Stat3 (cropped blots are shown, and original raw blots are shown in Supplementary Information Fig. 1). The degree of Stat3 activation was determined by dividing the density of p-Stat3 by that of total-Stat3 (n=5). One sample t-test was performed. ** $p<0.01$, *** $p<0.001$.

CD122/132 occurs at the cell surface. To test whether CD122/132 clustering of NK cells required co-localization into lipid rafts, as is the case with CD8$^+$ naïve T cells[8], we visualized lipid rafts by GM-1 staining (top panel, Fig. 4e). While GM-1 staining was uniformly distributed along the cell membrane, CD132 still formed distinct puncta (top panel, Fig. 4e), suggesting that CD122/CD132 clustering is not likely to be controlled by lipid rafts. However, NK cells treated with Latrunculin A, which inhibits F-actin polymerization, or nocodazole, which inhibits microtubule formation, demonstrated significantly lower levels of CD132 (bottom panel, Fig. 4e) suggesting that CD122/132 clustering is dependent on cytoskeletal reorganization.

To further confirm the role of homotypic interaction in IL-2 signaling, we measured the level of Stat3 activation downstream of CD122/CD132 clustering. As shown in Fig. 5a, NK cells in social microwells demonstrated bright staining of active phospho-Stat3 (p-Stat3), which overlapped with that of CD25. However, cells cultured in lonesome wells demonstrated weak p-Stat3 and CD25 staining, and their co-localization was significantly diminished. Similarly, NK cells cultured in round-bottom wells demonstrated elevated p-Stat3 at the protein level that was more than two fold higher than that seen among NK cells cultured in flat-bottom wells (Fig. 5b). These data clearly demonstrate that cell-cell contact among NK cells enhances the IL-2R-mediated intracellular signaling pathways leading to the activation of Stat3 and elevated cell proliferation.

2B4, but not LFA-1, is required for NK cell contact mediated activation and proliferation by IL-2. We next investigated the molecular basis in controlling NK cell-to-cell homotypic interactions. Among several receptors known to mediate cell-cell adhesion, LFA-1/ICAM-1 was shown to be most important for T cell activation and proliferation[9], whether this interaction plays a significant role in homotypic NK cell activation is unknown. Aside from LFA-1, 2B4, a SLAM family receptor member that binds to CD48, is ubiquitously expressed on NK cells and can regulate the activation and function of NK cells[10]. We therefore investigated if these receptors were localized at the NK-NK contact sites by immunofluorescence. Upon IL-2 activation, we found that both CD11a (LFA-1) and 2B4 localized to synapses along cell-cell contact sites. However, NKG2D, an NK activating receptor ubiquitously expressed on NK cells, was not found to be present at the NK-NK contact sites; rather it was clustered randomly throughout the cell (Fig. 6a).

To determine whether homotypic interactions of 2B4/CD48 or LFA-1/ICAM-1 receptor pairs among NK cells contribute to the IL-2-mediated activation of NK cells, we treated NK cells cultured in social or lonesome microwells with blocking antibodies. While the activation/proliferation burst observed in social wells was independent of LFA-1 signaling, treatment with an anti-2B4 blocking antibody inhibited the enhanced proliferation (Fig. 6b) and activation (Fig. 6c) of NK cells in social microwells down to levels seen in lonesome microwells. A similar defect was observed when 2B4KO NK cells were cultured in social microwells (Fig. 6b, c). In addition, anti-2B4-treatment reduced the level of CD122/CD132 clustering of NK cells in social microwells down to the level of NK cells in lonesome microwells (Fig. 6d). Of note, our previous study using plate-coated anti-2B4 and anti-CD48 antibodies revealed that triggering of 2B4, not CD48, enhanced cytokine responsiveness[11]. Therefore, enhanced IL-2 signaling following homotypic NK-NK cell interactions required 2B4 ligation and occurred at the level of IL-2R clustering at the surface.

We next examined if the contact-mediated control of NK cell activation was limited to IL-2 or extended to other common γ-chain receptor cytokines. Since IL-15 signaling also requires assembly of CD122 and CD132 and plays a critical role in NK cell activation[5,12], we tested whether 2B4 was required for IL-15-induced NK cell activation. Indeed, proliferation of NK cells by IL-15 was significantly enhanced in social microwells compared to that in lonesome wells, suggesting that cell-cell contact is necessary for optimal activation by IL-15. As in the case with IL-2, treatment with anti-2B4 mAb abrogated this effect (Fig. 6e). Taken together, our data demonstrate that the homotypic NK-to-NK cell interactions occur in the presence of common γ-chain cytokines, IL-2 and IL-15, and require 2B4/CD48 interaction.

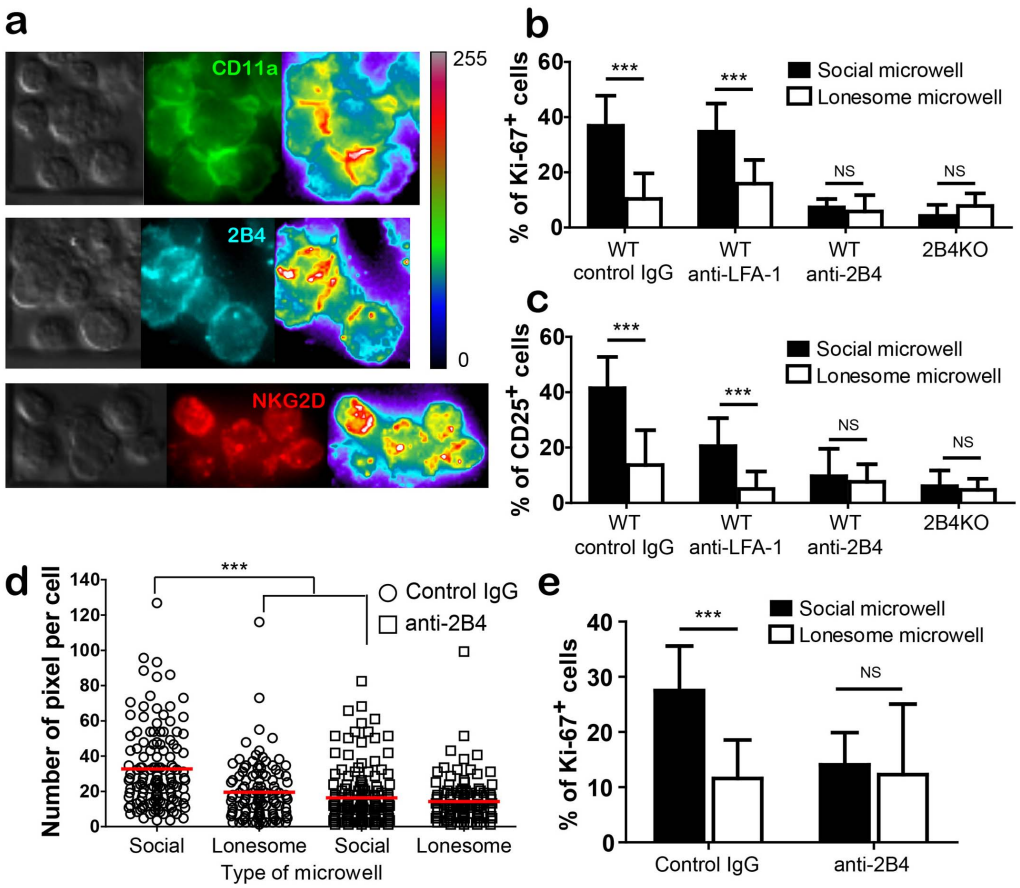

Figure 6 | 2B4-mediated cell-to-cell interaction is essential for contact-mediated augmentation of NK cell activation. (a) NK cells in microwells were treated with 500 U/ml of IL-2 for 18 h, fixed and stained with CD11a, 2B4, and NKG2D, and distribution of each molecule of NK cells in social microwells was examined. Representative DIC and fluorescence images of CD11a (top panel, green), 2B4 (middle panel, cyan) and NKG2D (bottom panel, red) are shown. (b-c) Blocking antibody for LFA-1 or 2B4 was added to WT NK cells in microwells at a final concentration of 10 μg/ml; alternatively 2B4 KO NK cells were plated onto microwells, treated with 500 U/ml of IL-2 for 36 h, fixed and stained with Ki-67 (b) and CD25 (c). (d) NK cells in microwells were treated with 500 U/ml of IL-2 for 18 h in the presence or absence of anti-2B4 (10 μg/ml), fixed and stained with anti-CD132, and clustering of CD132 was quantitatively analyzed. (e) NK cells in microwells were treated with IL-15 (10 ng/ml) for 30 hours in the presence or absence of anti-2B4 (10 μg/ml), fixed and stained with anti-Ki-67. Ki-67$^+$ cells were quantified as shown. Data are representative of 3 independent experiments. One sample t-test was performed. *** $p<0.001$.

2B4-mediated interaction enhances CD122/132 clustering and proliferation of NK cells in vivo. To validate if 2B4-mediated clustering of CD122/132 also occurs in vivo to augment proliferation of NK cells, we injected both WT and 2B4-KO mice with poly I:C, a TLR3 agonist that can induce the cytokine milieu seen with IL-2 or IL-15 *in vitro*[13,14], and measured CD122/132 clustering (Fig. 7a). We found that CD122 and CD132 clustered as bright puncta and colocalized in NK cells of WT mice activated with poly I:C (Fig. 7b). However, CD122 clustering in 2B4KO mice was significantly diminished to levels identical to that of NK cells in PBS-injected mice (Fig. 7c). These results demonstrate that 2B4-mediated clustering of CD122/132 in NK cells also occurs in vivo in response to cytokine stimulation. NK cell clustering of CD122/132 corresponded to the degree of cell proliferation, as measured by Ki-67 expression, and highlights the signaling defects in NK cell proliferation in 2B4 KO mice (Fig. 7d). Similar to in vitro results, percentage of Ki-67$^+$ NK cells from 2B4KO mice was significantly lower than WT mice. Therefore, 2B4-mediated homotypic NK cell-to-cell interactions play a critical role in the IL-2R signaling and synergistic proliferation of NK cells in response to γ-chain receptor cytokines *in vivo*.

Discussion

NK cells play a critical role at the interface between the innate and adaptive immune response in controlling infection and cellular transformation. The hierarchical program initiated by DCs leading to NK activation and full effector function has been shown to be essential to the resolution of these processes[15,16]. The data presented here establish a novel NK cell activation pathway that is controlled by homotypic cell-cell contact and cell clustering downstream of the initial crosstalk between DCs and NK cells. Using a cell-laden microwell approach combined with quantitative fluorescence microscopy, we confirmed that the local density of NK cells, and not merely the number of cells, controls the degree of NK cell activation and proliferation. Furthermore, cell-to-cell contact increased NK cell responsiveness to IL-2 and IL-15 signaling by initiating the IL-2R clustering process and Stat3 activation, leading to enhancement of NK cell activation and proliferation. Importantly, this process required intact actin and microtubules and was dependent on 2B4/CD48 interaction, but not LFA-1/ICAM-1. Taken together, our study sheds new light on a mechanism of NK cell activation that is dependent on homotypic cell-cell clustering regulated by 2B4/CD48 interaction.

The evidence provided here, that attaining full NK effector function and proliferation is a contact-dependent process mediated by 2B4, extends findings from our previous study demonstrating a direct effect of 2B4 on NK cells through CD48 binding on neighboring NK cells[10] and addresses a long-standing question of whether NK cells require co-stimulation to be optimally activated. In our study, both LFA-1 and 2B4 co-localized to NK contact sites upon IL-2

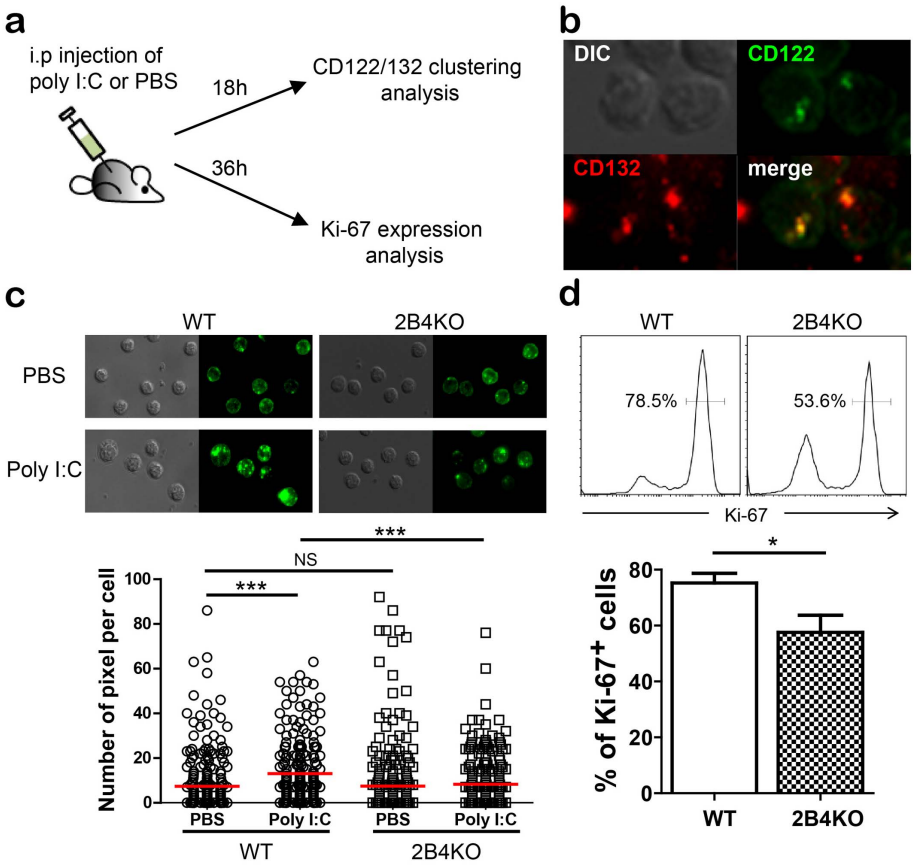

Figure 7 | Expression of 2B4 is critical for enhanced CD122/132 clustering and proliferation of NK cells in vivo. (a) Schematic illustration of in vivo experiments, as described in Methods. M. K drew this figure. (b) Representative DIC and fluorescence images of NK cells stained with anti-CD122 and anti-CD132 mAbs. NK cells ($CD3^-NK1.1^+$) purified from splenocytes of poly I:C- or PBS-injected mice 18 h after injection were fixed and stained, and fluorescence images were acquired. (c) Representative DIC and fluorescence images of NK cells stained with FITC-anti-CD122 mAbs (top) and quantification of CD122 clustering (bottom). Data are representative of three independent experiments. (d) Proliferation of NK cells in vivo assessed by Ki-67 expression. Splenocytes from WT or KO mice injected with PBS or poly I:C were harvested 36 h after injection, stained with anti-NK1.1, anti-CD3, and anti-Ki-67, and analyzed by flow cytometry. Representative histograms showing Ki-67 expression levels of NK cells ($CD3^-NK1.1^+$) with annotated percentages of $Ki\text{-}67^+$ cells (top panel), and bar graphs showing the percentages of $Ki\text{-}67^+$ cells per each condition. Data are representative of two independent experiments. One sample t-test was performed. * $p<0.05$, *** $p<0.001$.

stimulation, but the synergistic effect initiated by homotypic interaction appeared to depend exclusively on 2B4, and not LFA-1. We have shown previously that 2B4/CD48 binding results in unidirectional signaling through the 2B4, not CD48, bearing cells in response to IL-2 or type I interferon[10,11]. However, 2B4 is also known to serve as a functional switch mediating both stimulatory and inhibitory signals. This was shown to depend on the level of 2B4 surface expression and the adapter molecules bound to immune-receptor tyrosine-based switch motifs (ITSM) present on the intracellular domain of 2B4[17,18]. The stimulatory role for 2B4 described here and in our earlier study[10] and contrasts with the inhibitory role 2B4 plays in other cell types such as exhausted T cells[19–21], and NK cells themselves[22,23]. The precise mechanism responsible for these opposing functions is still not fully understood but one possibility is that the expression level of surface 2B4 may determine the outcome of engagement, with lower 2B4 levels leading to a stimulatory pathway[24] by recruiting the adapter molecule, SAP[18,25]. The fact that NK cell synergy following homotypic cell-cell contact can be more effectively abolished when 2B4/CD48 interaction was blocked during the early phase of this process when 2B4 expression is low, but not during or after the initial cell contact has been established, is consistent with a surface proximal event.

Following 2B4 engagement, we observed enhanced responsiveness to IL-2 and IL-15, common γ chain receptor cytokines. The mechanism by which 2B4 engagement leads to an amplified IL-2 signal will require further study but possible scenarios are proposed. Since binding of SAP to ITSMs (immunoreceptor tyrosine-based switch motifs)[26] can lead to activation of PLC-γ through recruitment of effector tyrosine kinases, e.g., fyn[27–30], 2B4/CD48 binding following homotypic cell-cell contact may synergize with IL-2 signaling at the membrane proximal step involving PLC-γ activation or further downstream along the Ras/MAP kinase activation pathway[31]. Another mutually non-exclusive possibility is that soluble IL-2 (or IL-15) present in limiting amounts within the microenvironment may be sequestered and concentrated locally at cell-cell contact sites. Since homotypic cell-cell contact leads to rapid upregulation of surface CD25, soluble IL-2 may be trans-presented to neighboring NK cells. IL-2 trans-presentation by NK cells has not previously been reported, but our preliminary data demonstrating that CD25 is required to deliver an IL-2 signal through NK-NK contact supports this concept. 2B4/CD48 interaction may further stabilize cell-cell contacts, or additionally facilitate the proliferation and expansion process by inhibiting NK cell fratricide[23,32]. This is a feature observed only with 2B4 and not LFA-1, although both molecules can function as adhesion receptors and trigger intracellular signaling.

Our data provide clear evidence that the 2B4-mediated signaling in NK cells through homotypic NK-NK cell interactions plays an important role in augmenting cytokine receptor clustering and proliferation

both in vitro and in vivo. Considering that CD48 is expressed in many different types of hematopoietic cells, we do not exclude the possibility that 2B4 signaling in NK cells may be induced by heterotypic interactions with CD48-expressing non-NK cells including T cells[33] as well as by homotypic interactions with neighboring NK cells. Direct observation of cellular dynamics during priming by in vivo multi-photon microscopy may be helpful for the formal demonstration of NK-NK homotypic interactions in vivo. In case of T cells, formation of dynamic multi-cellular clusters with significantly increased duration of T cell-T cell contacts during activation, which significantly enhance cytokine signaling and differentiation, was demonstrated for both CD4 and CD8 T cells[9,14,15]. Careful examination of NK-NK contact duration in WT and 2B4 KO mice would provide a clue about significance of 2B4/CD48 in NK-NK homotypic interactions *in vivo*. However, prolonged cell-cell contact may not be necessary for cell-cell communication in immunity since T cells interacting with APC presenting self-peptide receive tonic signals that significantly lower activation threshold of T cells[34–36] without forming stable cell-cell contacts[37]. Therefore, functional in vivo study with CD48 present only in NK cells would be the most definitive method to verify in vivo relevance of NK-NK homotypic interactions mediated by 2B4-CD48 interactions demonstrated in vitro in the current study.

In terms of addressing the broader question of why cell contact between NK cells is necessary for optimal NK cell activation in the normal immune response, one possibility is that cell contact acts as a quorum-sensing mechanism, whereby the density of activated NK cells within an affected area can function as a measure of the extent of viral infection or tumor transformation. In a recent study, NK cells were shown to be present in the tumor microenvironment in isolation under steady-state conditions but upon expression of an NK activating ligand on tumor cells, a dramatic increase in the number and density of NK cells was detected within the tumor environment[38] wherein homotypic contact is more likely to occur. In our study, intimate cell-to-cell contact among NK cells that cluster following initial activation provide potent costimulatory signals to each other through 2B4 and mediate IL-2 receptor upregulation and trans-presentation of local IL-2 to nearby NK cells. This may be physiologically relevant in vivo. During the initial phases of the innate response, activated DCs induce rapid clustering of NK cells[39] followed by DC-derived IL-2 priming[40]. NK cell clustering and homotypic interaction lead to upregulation of IL-2 receptor expression and IL-2 trans-presentation further expanding a self-propagating NK population independent of other APCs. Since NK cells can also participate as antigen-presenting cells whereby exogenous antigen is actively internalized, processed and presented to T cells[41], there exists a potential dual role for activated NK cells to present *both* IL-2 and antigen to the emerging adaptive immune response.

The revelation that homotypic NK cell-to-cell contact may be involved in choreographing the interaction between NK cells, IL-2 and elements of innate and adaptive immunity in a 2B4-dependent manner highlights the physiologic cell-to-cell communication process in vivo. Any physiologic events that alter local cytokine levels, NK cell density or 2B4 signaling can have a significant impact on the cascade of events leading to full NK cell activation and proliferation and the control of infection and tumor immunity.

Methods

Mice. Six to 8 week old female C57BL/6 mice were purchased from Nara Biotech (Seoul, Korea) and Frederick Cancer Research and Developmental Center (National Cancer Institute, Frederick, MD). 2B4 knock-out mice were generated as previously described[22]. All mice were maintained at the University of Chicago and Korea University animal housing facilities under specific pathogen-free condition. All animal experiments were approved by Institutional Animal Care and Use Committees of University of Chicago and Korea University and performed in accordance with national and institutional guidelines.

Primary mouse NK cell preparation. Purification of NK cell was performed as previously described[42]. NK cells were enriched from spleen cell suspensions via negative depletion of B cells by passing through a nylon wool column followed by magnetic depletion of CD3, CD4, CD8, CD19 and Gr-1 positive cells using miniMACS according to the manufacturer's protocols (Miltenyi Biotec, Bergisch Gladbach, Germany). The purity of $CD3^-DX5^+$ NK cells was 82-95%. Enriched NK cells were cultured in complete RPMI with IL-2 (rhIL-2; Chiron, Emeryville, CA).

Antibodies and Flow cytometry. Anti-mouse NK1.1 (clone PK136), CD3 (145-2C11), CD69 (H1.2F3), CD25 (PC61.5), CD122 (TM-b1), CD132 (TUGh4), NKG2D (CX5), 2B4 (ebio244F4), CD48 (HM48-1), CD2, Trail (N2B2), NKp46 (29A1.4), ICAM-1 (ebioKAT-1), granzyme B (NGZB), perforin (eBioOMAK-D), T-bet (4B10), anti-Ki-67 (B56), CD44 (IM7) and functional grade anti-CD11a (M17/4) monoclonal antibodies were purchased from ebioscience (San Diego, CA, USA) and BD Biosciences (San Diego, CA, USA). Purified rat IgG was purchased from Jackson Immunoresearch (West Grove, PA, USA). Purified streptavidin was obtained from Invitrogen. PI and Annexin V (BD Biosciences) were per manufacturer's instructions. Flow cytometry was performed with a FACSCalibur (BD Biosciences), LSRFortessa (BD Bioscience), MoFlo XDP (Beckman Coulter) and the data were analyzed with CellQuest software (BD Biosciences) and FlowJo (version 7.6.5). Proper live lymphocyte population was gated by forward-/side-scatter and PI negative staining.

CFSE dilution assay. Purified NK cells suspended in RPMI media were labeled with 5 μM CFSE at 37°C for 10 minutes. Cells were washed twice in PBS, and CFSE-labeled NK cells were incubated with 96 well flat-bottom or round-bottom plate with 300–500 U/ml rIL-2. After incubation, NK cells were harvested and assayed. Flow cytometry was performed with a FACSCalibur and analyzed with CellQuest software (BD Bioscience).

^{3}H-Thymidine incorporation assay. ^{3}H-thymidine incorporation assay was performed as previously described[43]. Cell viability was determined by Trypan Blue exclusion. To assess DNA synthesis, cells were exposed to 1 μCi/ml ^{3}H-thymidne (Amersham Pharmacia Biotech, Korea) for 18 hours. Cells were harvested with Micro96 harvester (Skatron, Norway) and disintegrations per minute (DPM) counted by a β-counter (Packard Instrument Company, Meriden, CT).

CD107a granule release assay and IFN-g intracellular staining. NK cells, cultured as described above, were admixed with YAC-1 cell line at an E:T ratio of 1 : 1 in a round-bottom 96-wells plate for one hour. Anti-CD107a mAb conjugated with FITC was added in the presence of Golgistop (BD Biosciences) for 5 hours. After incubation, samples were stained with anti-NK1.1 and anti-CD3 Ab, fixed and permeabilized using cytofix/cytoperm intracellular stainig kit (BD Biosciences) and then stained with anti-IFN-γ-PE Ab. Flow cytometry was performed with FACSCalibur (BD Biosciences) and analyzed using CellQuest software (BD Biosciences).

Western blot analysis. NK cells were harvested after 14 hour incubation with rIL-2 and lysed with protein lysis buffer (20 mM Tris, pH 7.5, 100 mM NaCl, 5 mM $MgCl_2$, 1% Nonidet P-40, 0.5% sodium deoxycholate) supplemented with protease and phosphatase inhibitor cocktail PhosSTOP (Roche Diagnostics, Rotkreuz, Switzerland). Cell lysates were loaded onto SDS-PAGE and transferred to (PDVF) membrane (Gelman, Arbor, MI). This membrane was blocked with 5% skim milk in TBST overnight at 4°C and probed with anti-mouse phospho-Stat3 (Tyr 705; 79/86 kDa) or anti-Stat3 (92 kDa, Cell Signaling Technology, Danvers, MA, USA). After incubation with HRP (Jackson ImmunoResearch Laboratories, West Grove, PA, USA), immunoreactive proteins were visualized using SuperSignal West Pico chemiluminescent substrate (Pierce, Rockford, IL, USA). Band densitometry was performed using LabWorks (BioImaging Systems, UVP, Cambridge, UK).

PDMS mold fabrication. Micropatterned silicon masters were fabricated at POSTECH National Center for Nanomaterials Technology (NCNT) by standard photolithography using 7 μm thick AZ 1512 (MicroChem) positive photoresist films on silicon wafer. Sylgard 184 pre-polymer base and curing agent (Dow chemical) were casted onto the silicon masters and cured 1 h at 70°C. Then, cured PDMS were peel off, and cut to create open channels.

NK cell-laden hydrogel microwell fabrication. Hydrogel microwells were constructed as described previously[7]. Briefly, glass surfaces were functionalized with biotin and acrylate groups. Hydrogel microwells were created on the dual-functionalized glass surfaces by perfusing precursor solution (Poly(ethylene glycol) dimethacrylate) to the open channels and curing precursor solutions with UV. Then, the floors of the hydrogel microwells were coated with a capturing antibody by adsorbing streptavidin and subsequently adsorbing biotinylated anti-CD44. Then, 200 μL suspension of naive NK cells (2×10^7 cells/ml) was applied to the anti-CD44 functionalized microwells and incubated at 4°C for 1 hour with gentle shaking. By gently washing cell-seeded dishes with cold PBS, we could remove non-adhering and weakly adhering cells by non-specific interactions, and obtain cellular arrays of NK cells in hydrogel microwells.

Immunofluorescence microscopy of cells in microwells. Purified NK cells were plated into the microwells and stimulated with rIL-2 for 18–36 hours at 37°C, 5% CO_2, and fixed and stained for immunofluorescence microscopy. Briefly, cells in the microwell were fixed with 1% paraformaldehyde for 15 min at 4°C and permeabilized for 30 min with 0.02% saponin (Sigma) in PBS if necessary. Then, cells were incubated for 60 min with primary antibodies, washed and stained with secondary

antibody for 60 min. A modified Zeiss Axio Observer.Z1 epi-fluorescence microscope with 40X (Plan-Neofluar, NA=1.30) objective lenses and a Roper Scientific CoolSnap HQ CCD camera was used for imaging. XBO 75 W/2 Xenon lamp (75 W, Osram) and DAPI (EX. 365, BS 395, EMBP445/50), eGFP (EX BP 470/40, BS 495, EMBP 525/50), Cy3 (EX BP 550/25, BS 570, EMBP 605/70), and Cy5 (EX BP 620/60, BS 660, EMBP 770/75) filter sets were used for fluorescence imaging. Fluorescence images of fixed and stained NK cells were acquired by optical z-sectioning (25 individual planes, 0.5 μm apart). Integrated intensities of each molecule along the z-axis were obtained with ImageJ (NIH) and Metamorph (Molecular Devices). For quantification of CD122/132 puncta, identical thereshod values were applied to all the integrated images and numbers of pixels exceeding the threshold values were counted. Colocalization assay was performed using 'colocalization' plug-in of ImageJ.

Analysis of CD122/132 clustering and proliferation of NK cells in poly I:C challenged mice. WT or 2B4KO mice were injected with 200 μg of poly I:C (invivogen) or PBS. To assess clustering of CD122/132 of NK cells in vivo, splenocytes were harvested from the mice 18 h after injection, stained with anti-CD3, anti-NK1.1, and NK cells ($CD3^{-}NK1.1^{+}$) were sorted by MoFlo XDP (Beckman Coulter). Sorted NK cells were seeded onto anti-CD44-coated glass plates for 30 min at 4°C, washed briefly with PBS, fixed with 1% paraformaldehyde, and stained with APC-anti-CD122 and PE-anti-CD132 for 1 h at RT. Fluorescence images of the fixed and stained NK cells were acquired and quantitatively analyzed as described above. To assess proliferation of NK cells, splenocytes were harvested from the mice 36 h after injection, stained with anti-CD3, anti-NK1.1, and anti-Ki-67. Flow cytometry was performed with LSR Fortessa (BD Bioscience) and analyzed using FlowJo (version 7.6.5).

1. Smyth, M. J., Hayakawa, Y., Takeda, K. & Yagita, H. New aspects of natural-killer-cell surveillance and therapy of cancer. *Nat. Rev. Cancer.* **2**, 850–861 (2002).
2. Sun, J. C. & Lanier, L. L. NK cell development, homeostasis and function: parallels with CD8 T cells. *Nat. Rev. Immunol.* **11**, 645–657 (2011).
3. Lanier, L. L. Up on the tightrope: natural killer cell activation and inhibition. *Nat. Immunol.* **9**, 495–502 (2008).
4. Trinchieri, G. *et al.* Response of resting human peripheral blood natural killer cells to interleukin 2. *J. Exp. Med.* **160**, 1147–1169 (1984).
5. Chiossone, L. *et al.* Maturation of mouse NK cells is a 4-stage developmental program. *Blood* **113**, 5488–5496 (2009).
6. Alter, G., Malenfant, J. M. & Altfeld, M. CD107a as a functional marker for the identification of natural killer cell activity. *J. Immunol. Methods.* **294**, 15–22 (2004).
7. Doh, J., Kim, M. & Krummel, M. F. Cell-laden microwells for the study of multicellularity in lymphocyte fate decisions. *Biomaterials* **31**, 3422–3428 (2010).
8. Cho, J. H., Kim, H. O., Surh, C. D. & Sprent, J. T cell receptor-dependent regulation of lipid rafts controls naive CD8+ T cell homeostasis. *Immunity* **32**, 214–226 (2010).
9. Sabatos, C. A. *et al.* A synaptic basis for paracrine interleukin-2 signaling during homotypic T cell interaction. *Immunity* **29**, 238–248 (2008).
10. Lee, K. M. *et al.* Requirement of homotypic NK-cell interactions through 2B4(CD244)/CD48 in the generation of NK effector functions. *Blood* **107**, 3181–3188 (2006).
11. Kim, E. O. *et al.* Unidirectional signaling triggered through 2B4 (CD244), not CD48, in murine NK cells. *J. Leukoc. Biol.* **88**, 707–714 (2010).
12. Mortier, E. *et al.* Macrophage-and dendritic-cell-derived interleukin-15 receptor alpha supports homeostasis of distinct CD8+ T cell subsets. *Immunity* **31**, 811–822 (2009).
13. Alexopoulou, L., Holt, A. C., Medzhitov, R. & Flavell, R. A. Recognition of double-stranded RNA and activation of NF-κB by Toll-like receptor 3. *Nature* **413**, 732–738 (2001).
14. Doh, J. & Krummel, M. Immunological synapses within context: patterns of cell-cell communication and their application in TT interactions. *Curr. Topics in Microbiol. Immunol.* **340**, 25–50 (2010).
15. Gérard, A. *et al.* Secondary T cell-T cell synaptic interactions drive the differentiation of protective CD8+ T cells. *Nat. Immunol.* **14**, 356–365 (2013).
16. Biron, C. A., Nguyen, K. B., Pien, G. C., Cousens, L. P. & Salazar-Mather, T. P. Natural killer cells in antiviral defense: function and regulation by innate cytokines. *Annu. Rev. Immunol.* **17**, 189–220 (1999).
17. Sidorenko, S. P. & Clark, E. A. The dual-function CD150 receptor subfamily: the viral attraction. *Nat. Immunol.* **4**, 19–24 (2003).
18. Morra, M. *et al.* Structural basis for the interaction of the free SH2 domain EAT-2 with SLAM receptors in hematopoietic cells. *EMBO J* **20**, 5840–5852 (2001).
19. Blackburn, S. D. *et al.* Coregulation of CD8+ T cell exhaustion by multiple inhibitory receptors during chronic viral infection. *Nat. Immunol.* **10**, 29–37 (2009).
20. Raziorrouh, B. *et al.* The immunoregulatory role of CD244 in chronic hepatitis B infection and its inhibitory potential on virus-specific CD8+ T-cell function. *Hepatology* **52**, 1934–1947 (2010).
21. West, E. E. *et al.* Tight regulation of memory CD8(+) T cells limits their effectiveness during sustained high viral load. *Immunity* **35**, 285–298 (2011).
22. Lee, K. M. *et al.* 2B4 acts as a non–major histocompatibility complex binding inhibitory receptor on mouse natural killer cells. *J. Exp. Med.* **199**, 1245–1254 (2004).
23. Waggoner, S. N., Taniguchi, R. T., Mathew, P. A., Kumar, V. & Welsh, R. M. Absence of mouse 2B4 promotes NK cell-mediated killing of activated CD8+ T cells, leading to prolonged viral persistence and altered pathogenesis. *J. Clin. Invest.* **120**, 1925–1938 (2010).
24. Chlewicki, L. K., Velikovsky, C. A., Balakrishnan, V., Mariuzza, R. A. & Kumar, V. Molecular basis of the dual functions of 2B4 (CD244). *J. Immunol.* **180**, 8159–8167 (2008).
25. Sayos, J. *et al.* The X-linked lymphoproliferative-disease gene product SAP regulates signals induced through the co-receptor SLAM. *Nature* **395**, 462–469 (1998).
26. Bida, A. T. *et al.* 2B4 utilizes ITAM-containing receptor complexes to initiate intracellular signaling and cytolysis. *Mol. Immunol.* **48**, 1149–1159 (2011).
27. Bloch-Queyrat, C. *et al.* Regulation of natural cytotoxicity by the adaptor SAP and the Src-related kinase Fyn. *J. Exp. Med.* **202**, 181–192 (2005).
28. Kim, H. S., Das, A., Gross, C. C., Bryceson, Y. T. & Long, E. O. Synergistic signals for natural cytotoxicity are required to overcome inhibition by c-Cbl ubiquitin ligase. *Immunity* **32**, 175–186 (2010).
29. Tassi, I. & Colonna, M. The cytotoxicity receptor CRACC (CS-1) recruits EAT-2 and activates the PI3K and phospholipase Cgamma signaling pathways in human NK cells. *J. Immunol.* **175**, 7996–8002 (2005).
30. Wang, D. *et al.* Phospholipase Cgamma2 is essential in the functions of B cell and several Fc receptors. *Immunity* **13**, 25–35 (2000).
31. Colonna, M. Fine-tuning NK cell responses: it's a family affair. *Nat. Immunol.* **6**, 961–962 (2005).
32. Taniguchi, R. T., Guzior, D. & Kumar, V. 2B4 inhibits NK-cell fratricide. *Blood* **110**, 2020–2023 (2007).
33. Assarsson, E. *et al.* NK cells stimulate proliferation of T and NK cells through 2B4/CD48 interactions. *J. Immunol.* **173**, 174–180 (2004).
34. Stefanová, I., Dorfman, J. R. & Germain, R. N. Self-recognition promotes the foreign antigen sensitivity of naive T lymphocytes. *Nature* **420**, 429–434 (2002).
35. Hochweller, K. *et al.* Dendritic cells control T cell tonic signaling required for responsiveness to foreign antigen. *Proc. Natl. Acad. Sci. USA.* **107**, 5931–5936 (2010).
36. Römer, P. S. *et al.* Preculture of PBMCs at high cell density increases sensitivity of T-cell responses, revealing cytokine release by CD28 superagonist TGN1412. *Blood* **118**, 6772–6782 (2011).
37. Miller, M. J., Hejazi, A. S., Wei, S. H., Cahalan, M. D. & Parker, I. T cell repertoire scanning is promoted by dynamic dendritic cell behavior and random T cell motility in the lymph node. *Proc. Natl. Acad. Sci. USA.* **101**, 998–1003 (2004).
38. Deguine, J., Breart, B., Lemaitre, F., Di Santo, J. P. & Bousso, P. Intravital imaging reveals distinct dynamics for natural killer and CD8(+) T cells during tumor regression. *Immunity* **33**, 632–644 (2010).
39. Kang, S. J., Liang, H. E., Reizis, B. & Locksley, R. M. Regulation of hierarchical clustering and activation of innate immune cells by dendritic cells. *Immunity* **29**, 819–833 (2008).
40. Granucci, F. *et al.* A contribution of mouse dendritic cell-derived IL-2 for NK cell activation. *J. Exp. Med.* **200**, 287–295 (2004).
41. Hanna, J. *et al.* Novel APC-like properties of human NK cells directly regulate T cell activation. *J. Clin. Invest.* **114**, 1612–1623 (2004).
42. Pham, T. N. *et al.* Enhancement of antitumor effect using dendritic cells activated with natural killer cells in the presence of Toll-like receptor agonist *Exp Mol Med.* **42(6)**, 407–419 (2010).
43. Lee, S. *et al.* Expression and Function of TLR2 on CD4 Versus CD8 T Cells. *Immune Network.* **9(4)**, 127–132 (2009).

Acknowledgments

This work was supported by the Basic Science Research Program through the National Research Foundation of Korea (NRF) funded by the Ministry of Science, ICT, and Future planning (grant NRF-2007-00107 and NRF-2013M3A9D3045719) awarded to K.-M. Lee. and J. Doh is supported by a grant of the Korea Healthcare Technology R&D Project, Ministry for Health, Welfare and Family Affairs, Republic of Korea A121177/HI12C1079.

Author contributions

T.-J.K., M.K., V.K., J.D. and K.-M.L. designed the research; T.-J.K., M.K., H.-M.K., E.-O.K., K.K., K.-H.S., S.-A.L. and J.K. performed the experiments; T.-J.K., M.K., C.Y., J.D. and K.-M.L. analyzed the results; J.D., C.Y. and K.-M.L. wrote the manuscript.

Additional information

Supplementary information accompanies this paper at http://www.nature.com/scientificreports

Competing financial interests: The authors declare no competing financial interests.

How to cite this article: Kim, T.-J. *et al.* Homotypic NK cell-to-cell communication controls cytokine responsiveness of innate immune NK cells. *Sci. Rep.* **4**, 7157; DOI:10.1038/srep07157 (2014).